Vertical and Nonvertical Participation by Sulfur, Selenium, and Tellurium

Jonathan M. White,*[b] Joseph B. Lambert,*[a] Marisa Spiniello,[b] Scott A. Jones,[b] and Robert W. Gable[b]

Abstract: The mechanism of stabilization of positive charge on carbon by sulfur, selenium, or tellurium at the β-position has been investigated kinetically, by measurement of rate enhancements, and structurally, by variation of the bond strength to the leaving group. Stabilization can occur either nonvertically with formation of a bridged intermediate or vertically through hyperconjugation within an open carbocation. We observed large rate enhancements (10^5 for S, 10^6 for Se) in 97% aqueous trifluoroethanol with trifluoroacetate as the leaving group. These enhancements are consistent with either mechanism. Product structures also are consistent with either mechanism. Nine crystal structures revealed that the bond to the leaving group (C–O) is lengthened by the presence of S or Se at the β-position, in proportion to the basicity of the leaving group. This lengthening is not accompanied by angle distortions expected for the bridging mechanism. The crystallographic data support vertical (hyperconjugative) character along the reaction coordinate, more so for selenium than sulfur.

Keywords: anchimeric assistance · hyperconjugation · selenium · sulfur

Introduction

The ability of sulfur to assist in the intramolecular departure of nucleophilic leaving groups (nucleofuges) is a classic example of neighboring-group participation.[1, 2] Analogous behavior of the congeners of sulfur (selenium and tellurium) has been studied much less. The expected mechanism for S, Se, and Te, along with O, N, P, and the halogens, involves an intramolecular S_N2 displacement to produce **1** in Equation (1), in which M represents S, Se, or Te and X is the nucleofuge. The lone pair on these atoms serves as the nucleophile and provides the electrons to form the new σ bond. The reaction concludes with nucleophilic opening of the three-membered ring, usually to give a product of the type RM-CH_2CH_2-OH when water serves as the external nucleophile.

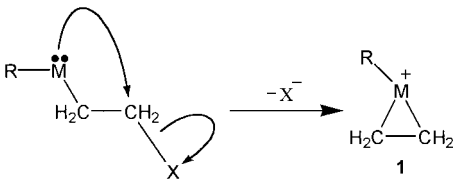

(1)

1

Silicon and its congeners (Ge and Sn) also can provide anchimeric assistance, but in these cases the σ electrons of the C–Si bond (C–Ge, C–Sn) fulfill the nucleophilic role played by the lone pair in Equation (1).[3, 4] Although a formally analogous mechanism can be written [Eq. (2a)], these lone-pair-free atoms have been shown to prefer another pathway [Eq. (2b)], in which ring closure does not occur. These two

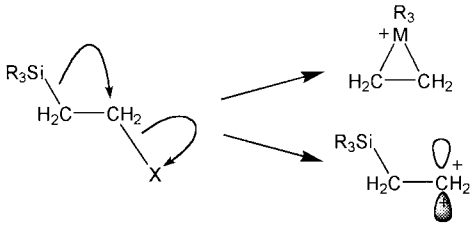

(2a)

(2b)

pathways have variously been called closed and open, bridged and nonbridged, or nonvertical and vertical [because the C–Si bond moves appreciably in Equation (2a) but is relatively stationary in Equation (2b)]. Proof of the vertical mechanism for stabilization by the C–Si bond and its congeners was based on stereochemistry, isotope effects, and NMR parameters of the stable ion.[4] Participation is driven by the high polar-

[a] Prof. J. B. Lambert
Department of Chemistry, Northwestern University
Evanston, Illinois 60208 (USA)
Fax: (+1) 847-491-5437
E-mail: jlambert@northwestern.edu

[b] Dr. J. M. White, M. Spiniello, S. A. Jones, Dr. R. W. Gable
School of Chemistry, University of Melbourne
Victoria 3010 (Australia)
Fax: (+61) 3-93475180
E-mail: white@oxygen.chemistry.unimelb.edu.au

  0947-6539/02/0812-2799 $ 17.50+.50/0

izability and electron-donating ability of the σ electrons in the C–Si bond.

The question thus arises whether participation in other long-established examples of anchimeric assistance actually occurs vertically rather than nonvertically. Traylor and co-workers[5] first raised this question, although they did not consider whether σ participation could compete effectively with n (lone pair) participation.

In the general case of atoms bearing lone pairs, vertical participation would occur by the mechanism shown in Equation (3) to give an unbridged cation **2**. The carbocation

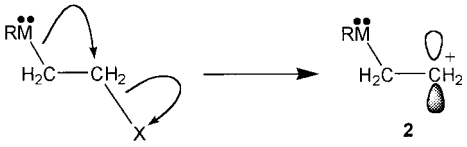

2 (3)

is stabilized by hyperconjugation (σ–π conjugation or double-bond/no-bond resonance, $RM{-}CH_2{-}CH_2^+ \rightleftharpoons RM^+\ CH_2{=}CH_2$). When atom M is a poor σ donor (because of low polarizability and high electronegativity), as is the case for the second row elements O, N, and F, we should expect normal anchimeric assistance of the type in Equation (1). For S, its congeners, and other atoms with high polarizability and low electronegativity (P and Br, for example), vertical stabilization [Eq. (3)] may be the preferred mechanism. We have examined the mechanistic alternatives for S, Se, and Te by kinetic and structural methods, and we report herein the results of that study.

Results

The kinetic method involves establishing the presence of anchimeric assistance as demonstrated by rate enhancement. We compare, under identical conditions, the rates of molecules containing the heteroatom M with the rate of an analogous molecule in which the entire heteroatom substituent is replaced by hydrogen, a nonparticipating atom. The result is a rate ratio, such as k_S/k_H for sulfur. The two systems must have the same molecular framework and the same geometry between the leaving group X and the participating entity.

Both vertical and nonvertical participation is maximal when the M-C-C-X dihedral angle is 180°, that is, antiperiplanar. Nonvertical participation then occurs by the standard backside displacement within this geometry, and vertical participation has optimal overlap within this geometry. Nonvertical participation falls off rapidly as the M-C-C-X dihedral angle decreases from 180°. Vertical participation, however, varies as the square of the cosine of the dihedral angle (this function allows strong overlap at the periplanar geometries, 0 and 180°, and zero overlap at the orthogonal geometry, 90°). Thus examination of antiperiplanar systems provides the maximal information about participation.

The most easily accessible system for obtaining this geometry is offered by the cyclohexyl framework with the diaxial stereochemistry, as in **3**. When R is *tert*-butyl, the molecule is constrained to remain almost entirely in the indicated geometry. When R is methyl, the conformational constraint is only partial. When R is small (H), the indicated diaxial geometry becomes disfavored, and the product of ring reversal, the diequatorial isomer, is preferred in a rapid equilibrium. According to the Winstein–Holness formalism, the observed rate is the populationally weighted average of the rates of the individual conformers. We have prepared several such systems and report the kinetics of solvolysis herein.

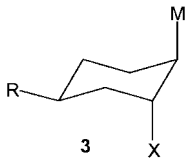

3

As rate enhancements are expected from either mechanism in the antiperiplanar molecule **3**, another approach is required to distinguish the mechanisms. In the case of Si, we used a variety of methods, including stereochemical variation and isotope effects.[4] One of the most successful of these methods is the *variable oxygen probe*, which detects the presence of electronic interactions between electron donors M and oxygenated leaving groups X in the ground state. The method was first applied to the generalized anomeric effect by Kirby and co-workers.[6] White and co-workers extended the method to the field of silicon participation.[7] The method involves low-temperature crystallography of a series of structures, in which the leaving group X is varied (X is either carboalkoxy or phenoxy). Electron demand of the leaving group is measured by the pK_a of the conjugate acid of the leaving group (carboxylate/carboxylic acid or phenoxide/phenol). The acids are selected to provide a range of pK_a's. The slope of the plot of the C–O bond length versus the pK_a of the acid provides a quantitative assessment of the ability of the group M to donate electrons to the leaving group. Because, of necessity, groups have not moved appreciably in the ground state except for bond lengthening, the slope of the plot is an indication of vertical participation. This assumption may be tested by searching for angle distortions that could be interpreted as movement along a reaction coordinate leading to bridging [Eqs. (1) and (2a)].

The slope for antiperiplanar Si (Si-C-C-X) was measured[7] to be -5.30×10^{-3}, whereas the slope for hydrogen[8] (H-C-C-X) was -2.91×10^{-3}. Although these differences ($5.30/2.91 = 1.8$) appear to be small, it should be kept in mind that they are logarithmic and, hence, represent exponents (e.g., a factor of two is equivalent to 10^2 kinetically, a factor of three to 10^3, and so on). The slope of -2.91 for H then is the baseline, characteristic of little or no vertical participation. The nearly twofold enhancement in slope for Si therefore is a strong structural response to the electron-withdrawing nature of X, reflecting movement along the reaction coordinate of Equation (2b) in the ground state and implying vertical participation by the C–Si bond. We report herein application of the variable oxygen probe to sulfur and its congeners.

Subjects for both kinetic and structural studies were prepared primarily from the biased trans alcohols **4a**–**4c**. Biasing is necessary for **4** in order to lock in the trans, diaxial conformation for kinetic studies. In some cases, isomer **5** with reversed regiochemistry and the unbiased *trans* isomer **6** also

  0947-6539/02/0812-2800 $ 17.50+.50/0 *Chem. Eur. J.* **2002**, *8*, No. 12

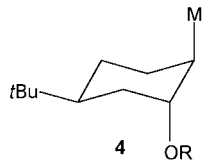

4

4a: M=SPh, R=H
4b: M=SePh, R=H
4c: M=TePh, R=H
4d: M=SPh, R=$COCF_3$
4e: M=SePh, R=$COCF_3$
4f: M=SPh, R=CO-4-$NO_2C_6H_4$

4g: M=SPh, R=CO-3,5-$(NO_2)_2$-C_6H_3
4h: M=SPh, R=CO-2,4-$(NO_2)_2$-C_6H_3
4i: M=SePh, R=4-$NO_2C_6H_4$
4j: M=SePh, R=CO-4-$NO_2C_6H_4$
4k: M=SePh, R=CO-2,4-$(NO_2)_2$-C_6H_3
4l: M=TePh, R=$COCH_3$

were studied. Methyl provides a useful locking device in the crystal, though not in solution. Thus we utilized derivatives **7** to provide further subjects for X-ray studies.

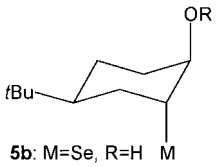

5b: M=Se, R=H

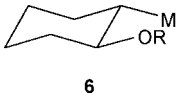

6

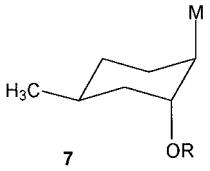

7

6a: M=SPh, R=H
6b: M=SePh, R=H
6c: M=TePh, R=H
6d: M=SPh, R=$COCF_3$
6e: M=SePh, R=$COCF_3$

7a: M=SPh, R=H
7b: M=SePh, R=H
7k: M=SePh, R=CO-2,4-$(NO_2)_2$-C_6H_3
7m: M=SPh, R=4-NO_2-C_6H_4

Systems **4a**–**4c** were prepared by reaction of *trans*-5-*tert*-butylcyclohexene oxide with sodium thiophenolate, sodium selenophenolate, and sodium tellurophenolate, respectively. The reverse regiochemistry in **5** was achieved by the same reaction with *cis*-5-*tert*-butylcyclohexene oxide. The unbiased *trans* systems **6** were obtained by the same reactions with cyclohexene oxide. The methyl systems **7** were prepared by the same reactions with *trans*-5-methylcyclohexene oxide.

For the solvolytic kinetic studies, the alcohols were converted to the trifluoroacetates, and rates were measured conductometrically for **4d, 4e, 6d**, and **6e**. Table 1 contains the absolute rates for the biased *trans* (**4**) and the unbiased *trans* (**6**) sulfur and selenium systems in 97% aqueous trifluoroethanol (TFE) at various temperatures. These rates produced activation parameters, from which the absolute and relative rates were calculated for 25 °C (Table 2). The relative rates are compared with cyclohexyl trifluoroacetate: k_M/k_H. The results of product of analyses are presented in the Experimental Section.

For the structural studies, the alcohols were converted to a series of carboxylic esters or phenoxides, and nine X-ray structures were obtained for **4f**–**4k, 4l, 7k**, and **7m**. When possible, structures were obtained at low temperature (130 K) to remove unwanted thermal effects. For **4h**, which underwent destructive phase changes at this temperature, the structure was determined at 200 K, and the structure of **4l** was determined at 173 K. Finally, **4g** underwent destructive phase changes below 273 K, so its structure was determined at room temperature. Crystallographic parameters may be found in the Experimental Section.

Table 1. Absolute rates for sulfur and selenium trifluoroacetates in 97% aqueous trifluoroethanol.

System	M	Stereochemistry	Temperature [°C]	k [s^{-1}]
4d	SPh	biased *trans*	41	5.55×10^{-4}
			51	1.355×10^{-3}
			61	3.47×10^{-3}
			66	5.75×10^{-3}
			71	9.11×10^{-3}
6d	SPh	*trans*	41	9.74×10^{-5}
			51	2.48×10^{-4}
			61	5.58×10^{-4}
			71	1.455×10^{-3}
4e	SePh	biased *trans*	0	5.4×10^{-4}
			9.5	1.51×10^{-3}
			17	3.7×10^{-3}
			26	8.5×10^{-3}
6e	SePh	*trans*	36	3.6×10^{-3}
			41	5.6×10^{-3}
			46	8.4×10^{-3}

Table 2. Absolute rates, relative rates, and activation parameters for sulfur and selenium trifluoroacetates in 97% aqueous trifluoroethanol.

	4d	**6d**	**4e**	**6e**
M	SPh	SPh	SePh	SePh
stereochemistry	biased *trans*	*trans*	biased *trans*	*trans*
k [s^{-1}] 25 °C	7.7×10^{-5}	1.80×10^{-5}	7.66×10^{-3}	1.33×10^{-3}
k_M/k_H[a]	1.1×10^5	2.6×10^4	1.1×10^7	1.9×10^6
E_a [kcal mol^{-1}]	20.31	19.40	17.28	16.48
log$A$	10.85	9.47	10.54	9.20
ΔS [e.u.]	−10.89	−17.2	−12.29	−18.45

[a] k_H is for cyclohexyl trifluoroacetate, 7.05×10^{-10} s^{-1} at 25 °C.

Selected bond lengths, angles, and dihedral angles are presented in Tables 3–5 for the sulfur derivatives, Tables 6–8 for the selenium derivatives, and Table 9 for the single tellurium compound. ORTEP drawings for representative structures are presented in Figures 1–4. Five of the nine structures (**4f, 4h, 4i, 4j, 7m**) consisted of two independent molecules (M1 and M2) in the asymmetric unit, differing by the dihedral angles around the Ph–M bonds C(*ortho*)-C(*ipso*)-M-C(ring). Tables 3–9 present data for both forms. Molecular mechanics calculations indicated that these conformations differ only slightly in energy and, therefore, are readily influenced by packing forces. The variable oxygen probe is manifested in plots of the C–O bond lengths versus the pK_a of the conjugate acid of the leaving group (Figure 5 for both sulfur and selenium).

Discussion

The presence of PhS at the β-position to the leaving group provides a rate enhancement of 1.09×10^5 when biased to the diaxial conformation (**4d**), in comparison with the analogous

Table 3. Selected bond lengths [Å] for PhS Structures.

	7m		4f		4g	4h	
	M1	M2	M1	M2		M1	M2
S1–Ar	1.784(2)	1.784(2)	1.7735(19)	1.7694(17)	1.759(3)	1.763(2)	1.7625(18)
S1–C2	1.830(2)	1.840(2)	1.8248(19)	1.8369(17)	1.811(2)	1.8244(19)	1.8234(18)
O1–C1	1.451(2)	1.451(2)	1.468(2)	1.468(2)	1.471(3)	1.4794(18)	1.4750(18)
C1–C2	1.534(3)	1.529(3)	1.523(3)	1.528(2)	1.516(4)	1.530(2)	1.529(2)
C2–C3	1.532(3)	1.529(3)	1.528(3)	1.524(2)	1.534(3)	1.527(3)	1.528(2)
C3–C4	1.524(3)	1.532(3)	1.531(3)	1.526(2)	1.524(4)	1.523(3)	1.520(2)
C4–C5	1.525(3)	1.526(3)	1.533(2)	1.532(2)	1.526(4)	1.535(3)	1.534(2)
C5–C6	1.529(3)	1.528(3)	1.534(2)	1.532(2)	1.534(3)	1.528(2)	1.530(2)
C1–C6	1.521(3)	1.523(3)	1.515(3)	1.523(2)	1.507(3)	1.511(2)	1.514(2)

Table 4. Selected bond angles [°] for PhS structures.

	7m		4f		4g	4h	
	M1	M2	M1	M2		M1	M2
CAr-S1-C2	101.31(9)	100.69(9)	104.71(8)	102.34(8)	107.37(12)	106.31(9)	105.88(8)
O1-C1-C6	105.67(15)	106.28(16)	108.47(14)	108.63(13)	104.89(18)	105.91(13)	104.36(13)
O1-C1-C2	109.30(15)	109.46(16)	104.25(14)	104.34(12)	108.37(19)	108.60(13)	109.81(13)
C1-C2-S1	110.55(13)	110.38(14)	111.84(13)	107.69(11)	112.16(18)	110.43(12)	109.47(12)
C3-C2-S1	108.41(14)	108.47(14)	107.31(12)	113.48(12)	106.15(18)	107.19(13)	107.91(12)
C3-C2-C1	112.12(16)	112.15(17)	110.49(15)	111.62(14)	110.1(2)	110.80(15)	111.15(14)
C4-C3-C2	113.33(17)	113.40(18)	112.64(15)	112.64(14)	112.9(2)	113.08(16)	112.37(15)
C3-C4-C5	111.50(17)	110.71(17)	112.33(14)	111.02(14)	111.8(2)	111.32(15)	111.32(14)
C4-C5-C6	109.74(17)	109.90(18)	109.25(15)	108.22(14)	108.6(2)	108.88(15)	108.45(14)
C1-C6-C5	113.38(17)	113.19(18)	113.29(15)	112.53(13)	113.4(2)	113.50(14)	112.92(14)
C6-C1-C2	112.70(16)	112.97(16)	113.91(14)	113.23(13)	113.8(2)	113.11(14)	112.78(13)

Table 5. Selected dihedral angles [°] for PhS structures.

	7m		4f		4g	4h	
	M1	M2	M1	M2		M1	M2
O1-C1-C2-C3	−69.5(2)	70.8(2)	67.28(17)	69.70(16)	65.9(2)	67.66(18)	−65.95(17)
S1-C2-C3-C4	72.7(2)	−72.3(2)	−70.09(17)	−71.30(16)	69.6(2)	−68.77(18)	68.03(17)
S1-C2-C1-C6	−73.45(18)	73.68(19)	68.72(17)	76.95(15)	−67.6(2)	69.01(17)	−69.14(16)
*C2-S1-C8-C13	110.49(17)	78.60(18)	32.46(18)	−150.81(13)	−175.10(19)	178.62(13)	10.54(18)
*C2-S1-C8-C9	−71.58(18)	−101.04(18)	−148.81(14)	31.14(16)	5.7(3)	−1.49(19)	−170.26(13)
C1-C2-C3-C4	−49.6(2)	49.9(2)	52.1(2)	50.61(19)	−52.0(3)	51.8(2)	−52.01(19)
C2-C3-C4-C5	54.6(3)	−55.2(3)	−55.9(2)	−57.4(2)	56.7(3)	−56.5(2)	57.2(2)
C3-C4-C5-C6	−56.3(2)	56.9(2)	54.6(2)	59.12(18)	−55.8(3)	56.2(2)	−57.82(19)
C4-C5-C6-C1	55.7(2)	−56.0(2)	−53.15(19)	−57.25(18)	54.6(3)	−55.26(19)	56.44(18)
C5-C6-C1-C2	−51.9(2)	51.5(2)	52.8(2)	52.92(19)	−53.6(3)	53.11(19)	−53.69(18)
C6-C1-C2-C3	47.7(2)	−47.4(2)	−50.8(2)	−48.24(19)	50.4(3)	−49.61(19)	49.97(18)
O1-C1-C2-S1	169.38(12)	−168.11(12)	−173.24(11)	−165.11(10)	176.20(14)	−173.72(11)	174.94(10)
C6-C1-C2-S1	−73.45(18)	73.68(19)	68.72(17)	76.95(15)	−67.6(2)	69.01(17)	−69.14(16)
O2=C-Ar-Ar′			−175.24(18)	152.77(16)	−172.7(2)	−164.02(17)	163.35(17)
O2=C-Ar-Ar″			5.0(3)	−24.4(2)	5.8(4)	17.5(2)	−18.9(2)

Table 6. Selected bond lengths [Å] for PhSe structures.

	4i		4j		7k	4k
	M1	M2	M1	M2		
Se1–Ar	1.925(3)	1.920(3)	1.916(2)	1.919(3)	1.912(4)	1.909(2)
Se1–C2	1.994(2)	1.976(2)	1.984(2)	1.976(3)	1.986(4)	1.976(2)
O1–C1	1.459(3)	1.453(3)	1.475(3)	1.474(3)	1.489(4)	1.474(2)
C1–C2	1.525(3)	1.520(3)	1.519(3)	1.512(4)	1.509(6)	1.525(2)
C2–C3	1.531(3)	1.525(3)	1.521(4)	1.530(4)	1.527(5)	1.528(2)
C3–C4	1.531(3)	1.536(3)	1.529(4)	1.526(4)	1.523(6)	1.526(2)
C4–C5	1.532(3)	1.535(4)	1.527(3)	1.532(4)	1.505(6)	1.537(2)
C5–C6	1.522(4)	1.524(4)	1.534(4)	1.536(4)	1.546(6)	1.536(2)
C1–C6	1.518(3)	1.521(3)	1.522(3)	1.514(4)	1.505(6)	1.517(2)

system with hydrogen in place of the sulfur functionality (this ratio corresponds to k_S/k_H) (Table 2) in 97% aqueous TFE at 25 °C. This value is seven orders of magnitude smaller than the enhancement found in the structurally analogous system for silicon ($k_{Si}/k_H = 2.4 \times 10^{12}$).[8] Two points are relevant in this comparison. First, the lower enhancement for sulfur is understandable in terms of their relative electronegativities (the Allred–Rochow values are 1.90 for Si and 2.58 for S). Silicon is clearly more electropositive and, hence, a better electron donor. Second, the presence of lone pairs on sulfur has conveyed no kinetic advantage, despite the presumed superior nucleophilicity of S lone pairs over simple, tetravalent Si. The kinetic differences thus may be understood entirely in terms of differences in the donor properties of the C–M bonds, without reference to the presence or absence of lone pairs. The simplest explanation thus invokes only the single mechanism of vertical participation [Eqs. (2b) and (3)]. This is not to say that the kinetic data exclude nonvertical participation [Eqs. (1) and (2a)], but they are entirely explicable without such a mechanism.

The rate enhancement for the unbiased system (**6d**) is a more modest 2.55×10^4, which compares with the ratio 9.5×10^8 for the analogous Si system.[9] The reduction for both unbiased systems comes from an admixture of the slower diequatorial form, in which the dihedral angle is approximately 60°. The fact that the enhancement is still very large comes from two factors. First, the diequatorial form is in equilibrium with the diaxial form. By the Winstein–Holness equation ($k_{obs} = N_a k_a + N_e k_e$, in which k_{obs} is the observed rate, N is the conformer population with a for axial and e for equatorial, and k is the conformer rate), a very large axial rate can offset a low equatorial rate, even if the axial proportion is small. If N_a is 0.1 for the unbiased equilibrium, then $N_a k_a$ still is about 10^4 for M = S (k_a may be approximated as the value for the biased form **4d**). Second, the equatorial rate may in fact be rather large. Thus, if

0947-6539/02/0812-2802 $ 17.50+.50/0 *Chem. Eur. J.* **2002**, *8*, No. 12

Table 7. Selected bond angles [°] for PhSe structures.

	4i		4j		7k	4k
	M1	M2	M1	M2		
CAr-Se1-C2	95.91(10)	96.13(10)	99.14(11)	101.65(11)	103.86(16)	100.41(7)
O1-C1-C6	106.2(2)	106.6(2)	108.5(2)	108.8(2)	105.7(3)	105.95(13)
O1-C1-C2	108.80(18)	107.97(19)	104.67(19)	104.3(2)	106.9(3)	105.79(12)
C1-C2-Se1	109.25(16)	109.60(16)	107.47(17)	111.5(2)	109.2(3)	106.54(11)
C3-C2-Se1	109.81(16)	111.03(16)	113.04(17)	107.50(19)	108.3(3)	112.43(12)
C3-C2-C1	113.1(2)	112.7(2)	112.1(2)	111.1(2)	111.1(3)	111.67(14)
C4-C3-C2	113.91(19)	113.3(2)	112.5(2)	112.1(2)	112.0(3)	112.42(14)
C3-C4-C5	107.58(19)	108.1(2)	111.7(2)	112.5(2)	111.5(3)	111.62(14)
C4-C5-C6	111.0(2)	112.1(2)	108.3(2)	109.4(2)	111.4(3)	108.57(13)
C1-C6-C5	112.9(2)	112.6(2)	112.8(2)	113.4(2)	113.4(3)	112.11(13)
C6-C1-C2	112.4(2)	112.3(2)	113.4(2)	114.0(2)	113.7(3)	113.56(14)

Table 8. Selected dihedral angles [°] for PhSe structures.

	4i		4j		7k	4k
	M1	M2	M1	M2		
O1-C1-C2-C3	72.1(2)	−68.4(2)	70.0(2)	67.9(3)	65.2(4)	66.4(2)
Se1-C2-C3-C4	−72.0(2)	70.3(2)	−71.7(2)	−69.9(3)	−65.4(4)	−69.4(2)
Se1-C2-C1-C6	77.3(2)	−75.3(2)	76.7(2)	69.3(3)	68.4(4)	73.77(14)
*C2-Se1-C8-C13	−110.2(2)	−63.6(2)	−149.7(2)	−148.2(2)	−9.2(4)	−170.61(14)
*C2-Se1-C8-C9	68.0(2)	118.4(2)	33.1(2)	32.6(3)	171.4(3)	9.5(2)
C1-C2-C3-C4	50.3(3)	−53.1(3)	50.0(3)	52.4(3)	54.5(4)	50.3(2)
C2-C3-C4-C5	−56.4(3)	56.0(3)	−56.4(3)	−55.9(3)	−56.7(5)	−56.0(2)
C3-C4-C5-C6	59.5(3)	−57.1(3)	58.1(3)	54.6(3)	53.5(4)	58.0(2)
C4-C5-C6-C1	−58.2(3)	55.8(3)	−56.2(3)	−52.3(3)	−50.2(5)	−56.7(2)
C5-C6-C1-C2	49.9(3)	−50.5(3)	52.4(3)	51.8(3)	49.3(5)	53.6(2)
C6-C1-C2-C3	−45.3(3)	48.8(3)	−48.1(3)	−50.6(3)	−51.0(4)	−49.3(2)
O1-C1-C2-Se1	−165.2814	167.44(14)	−165.17(15)	−172.18(16)	−175.4(2)	−170.44(9)
O2=C-Ar-Ar′			−23.6(4)	4.8(4)	20.6(5)	−79.1(2)
O2=C-Ar-Ar″			152.9(3)	−174.7(2)	−162.1(4)	100.5(2)

Table 9. Selected bond lengths [Å], angles [°], and dihedral angles [°] for **4l**.

Te1−Ar	2.1201(16)	O1-C1-C2-C3	−67.82(17)
Te1−C2	2.1866(16)	Te1-C2-C3-C4	68.93(17)
O1−C1	1.4732(19)	Te1-C2-C1-C6	−74.76(15)
C1−C2	1.527(2)	C2-Te1-C13-C18	−131.04(14)
C2−C3	1.522(2)	C2-Te1-C13-C14	47.78(14)
C4−C5	1.538(2)	C1-C2-C3-C4	−54.08(19)
C5−C6	1.538(2)	C2-C3-C4-C5	57.7(2)
C1−C6	1.525(2)	C3-C4-C5-C6	−54.72(19)
CAr-Te1-C2	94.47(6)	C4-C5-C6-C1	51.39(19)
O1-C1-C6	106.56(13)	C5-C6-C1-C2	−50.32(19)
O1-C1-C2	108.60(12)	C6-C1-C2-C3	50.26(18)
C1-C2-Te1	109.15(10)	O1-C1-C2-Te1	167.16(9)
C3-C2-Te1	112.72(12)		
C3-C2-C1	111.27(14)		
C4-C3-C2	111.87(14)		
C3-C4-C5	112.17(14)		
C4-C5-C6	109.22(14)		
C1-C6-C5	114.37(13)		
C6-C1-C2	113.12(13)		

N_a is 0.01 and $N_a k_a$ is about 10^3, contributions are necessary from the equatorial form to explain the observed rate. Significant rates are expected from the equatorial form only with the vertical mechanism. Whereas the backside displacement of the nonvertical mechanism is excluded in the *gauche* geometry of the diequatorial system, there is still considerable participation at 60° in the vertical mechanism because of the cosine-squared dependence.[9]

Selenium is superior to sulfur in terms of rate enhancement (Table 2). For the biased system (**4e**), the enhancement (k_{Se}/k_H) is 1.08×10^7, two orders of magnitude more than sulfur. For the unbiased case (**6e**), the enhancement is 1.88×10^6, also considerably larger. The high electropositivity (Allred–Rochow electronegativity 2.55) and (possibly more importantly) polarizability of selenium is responsible for its greater ability to participate, similar to the comparison between silicon and germanium (electronegativity 2.01). Examination of the activation parameters (Table 2) indicates that the faster rate for selenium is primarily enthalpic. The entropy of activation is actually slightly more negative for selenium, possibly due to higher solvation requirements. The faster rate for selenium is readily explained by the vertical mechanism, in which the higher donor ability of the C−Se bond provides stronger assistance.

To provide further insight into the nature of the solvolysis of the biased diaxial sulfur and selenium trifluoroacetates **4d** and **4e**, the products of the solvolysis in 97% aqueous TFE were determined. Solvolysis

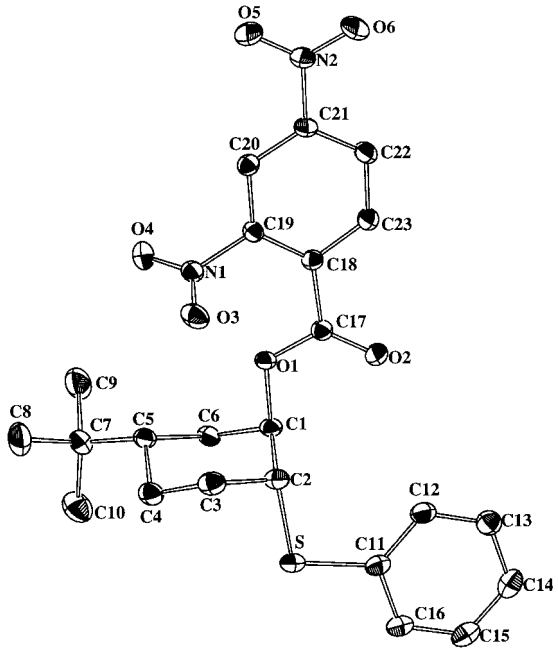

Figure 1. ORTEP structural diagram of *r*-5-*tert*-butyl-*c*-2-(phenylthio)cyclohexyl-*t*-yl 2,4-dinitrobenzoate (**4h**), with thermal ellipsoids drawn at the 30% probability level.

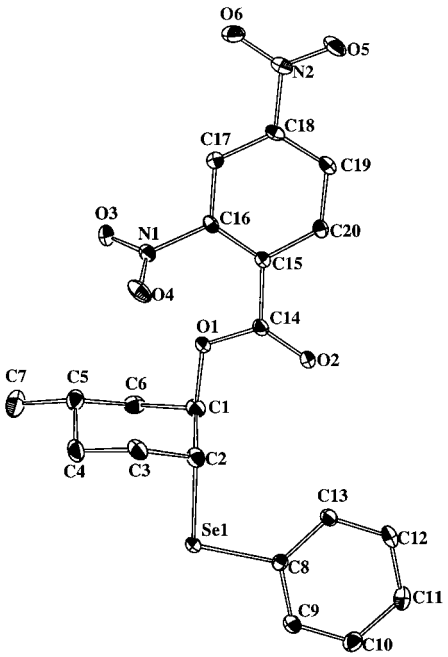

Figure 2. ORTEP structural diagram of *r*-5-methyl-*c*-2-(phenyselenyl)cyclohexyl-*t*-yl 2,4-dinitrobenzoate (**7k**), with thermal ellipsoids drawn at the 30% probability level.

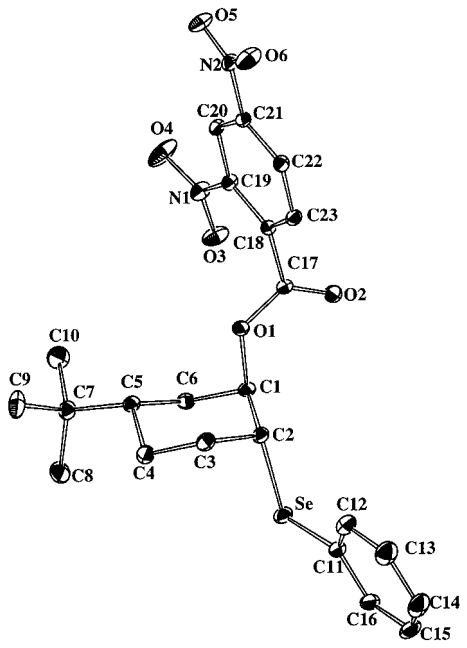

Figure 4. ORTEP structural diagram of *r*-5-*tert*-butyl-*c*-2-(phenylselenyl)-cyclohex-*t*-yl 2,4-dinitrobenzoate (**4k**), with thermal ellipsoids drawn at the 30% probability level.

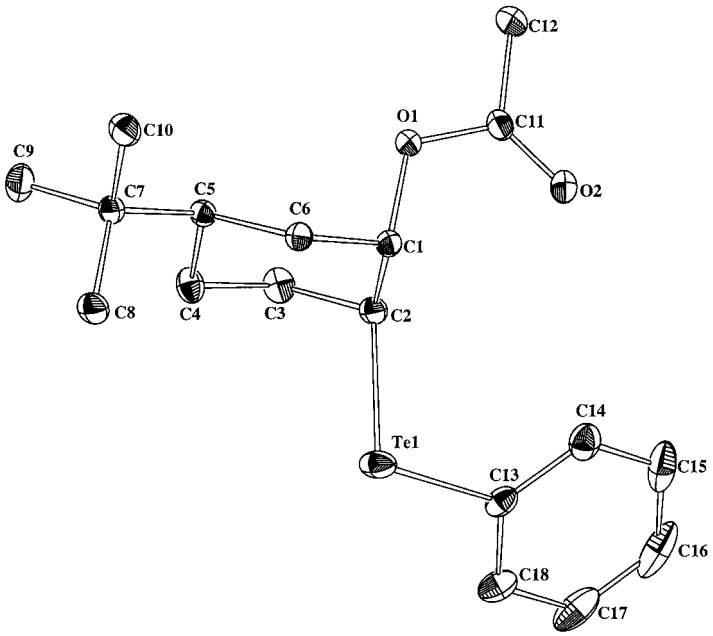

Figure 3. ORTEP structural diagram of *r*-5-*tert*-butyl-*c*-2-(phenyltelluryl)-cyclohex-*t*-yl acetate (**4l**), with thermal ellipsoids drawn at the 30% probability level.

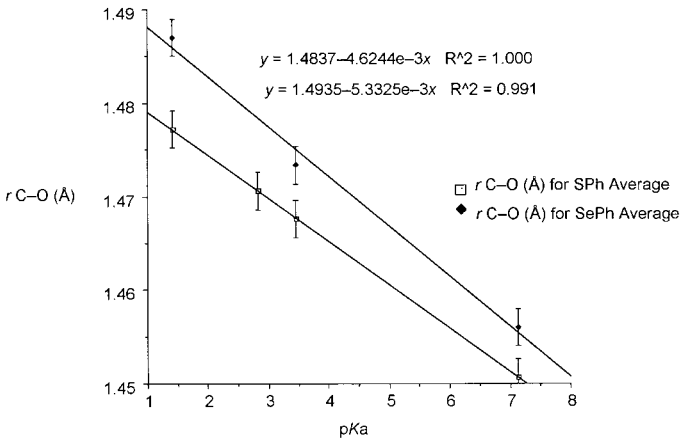

Figure 5. The variable oxygen probe, plotted as the C–O bond length versus the pK_a of the conjugate acid of the leaving group. The upper line is for selenium systems and the lower line for sulfur systems. The lines are least square fits to the data.

of the biased anti sulfur trifluoroacetate **4d** in this solvent for 12 hours at room temperature gave a 100% quantitative yield of the corresponding alcohol **4a.** Production of **4a** implies that solvolysis of **4d** occurs with retention of configuration. This outcome can be rationalized by invoking either the vertical or the nonvertical pathways shown in Scheme 1. Solvolysis by the vertical pathway involves the open cation in which it can be argued that the PhS group sterically shields the top face of the carbocation p orbital. Attack of H_2O from the bottom face

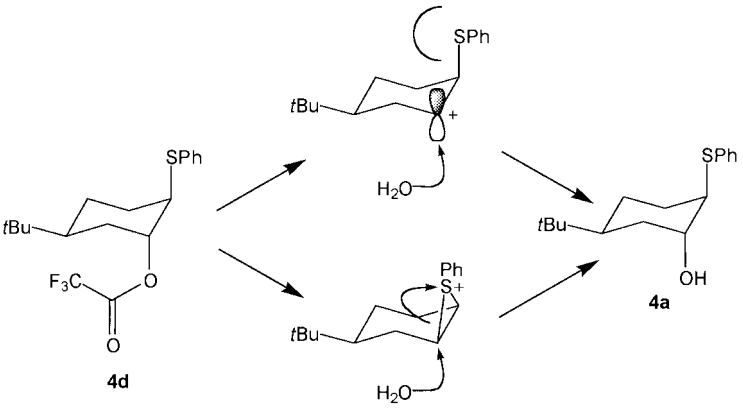

Scheme 1.

  0947-6539/02/0812-2804 $ 17.50+.50/0 *Chem. Eur. J.* **2002**, *8*, No. 12

gives the product **4a** with retention of configuration. Solvolysis by the nonvertical pathway involves the bridged intermediate, in which *trans*-diaxial ring opening by H_2O should occur via the more favored chair-like transition state (**8a**) giving **4a**.

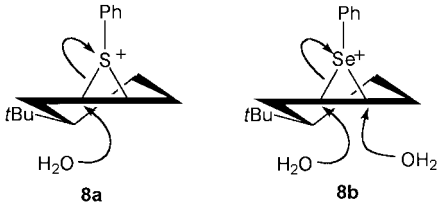

Solvolysis of the biased selenium trifluoroacetate **4e** gave an essentially quantitative conversion to an approximate 1/1.2 mixture of the alcohols **4b** and **5b** (Scheme 2). Other stereoisomers are present at less than 5%. A plausible mechanism

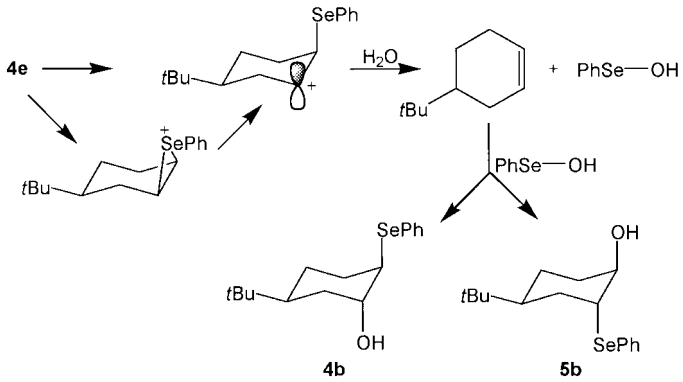

Scheme 2.

to account for the formation of both **4b** and **5b** involves formation of an intermediate carbocation, either directly by the vertical pathway or indirectly by the nonvertical pathway. Hyperconjugative stabilization of the carbocation by the phenylseleno substituent should render selenium susceptible to nucleophilic attack by H_2O, resulting in deselenation to give a mixture of 4-*tert*-butylcyclohexene and phenylselenol. Addition of phenylselenol to 4-*tert*-butylcyclohexene is expected to occur in a *trans*, diaxial fashion[10, 11] to give the observed mixture of **4b** and **5b**. Moreover, product **5b** is impossible to obtain from the nonvertical mechanism [Eq. (1)]. In order to maintain the required diaxial geometry for ring opening (see the alternative arrow in structure **8b**), the *tert*-butyl group would end up axial. In addition, the *tert*-butyl and phenylseleno groups would be *cis* to each other, contrary to the observation with **5b**. Further support for the mechanism of Scheme 2 is provided by the observation that solvolysis of **4d** in 97% aqueous TFE presence of a tenfold excess of cyclohexene (as a trapping agent) gave rise to a mixture of *trans*-2-(phenylselenyl)cyclohexanol and 4-*tert*-butylcyclohexene (Scheme 3). Such trapping of a cleaved selenium electrophile by a different alkene has been observed previously.[12]

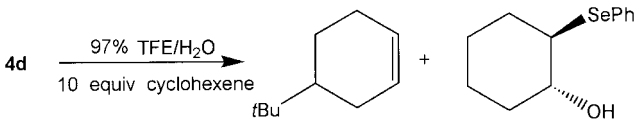

Scheme 3.

There is an important distinction between the products from the solvolysis of β-Si/Ge/Sn (elimination to form alkenes)[3, 4] and from the solvolysis of β-S/Se (substitution to form the alcohol). There are major differences in the mechanism that can occur after the rate-determining formation of the β-stabilized carbocation [Eqs. (2b) and (3)]. For Si, Ge, and Sn the subsequent step undoubtedly is reaction of oxygen nucleophiles with the substituent (Me_3M) to form the strong Si–O (etc.) bond irreversibly. We have presented evidence above that for Se the reaction proceeds to give PhSeOH by elimination, and this material is known to add back to double bonds to give the observed β-selenyl alcohols. Although a similar process could occur with S (through PhSOH), we believe that it is more likely that the lower ability of S to hyperconjugate leads to less positive charge on S and a lower tendency for nucleophiles to attack it and bring about elimination. The implied extrusion of phenylselenol from **4e**, but not of phenylthiol from **4d**, suggests there is less open cationic character in the reaction pathway for the sulfides than for the selenides, in agreement with their differences in electronegativity and polarizability.

The kinetic and particularly the product results are consistent with vertical participation. The data do not, however, exclude nonvertical participation, which can explain both rate enhancements and product structures. Consequently, we sought further evidence by application of the variable oxygen probe.

A key structural distinction is whether there is angular distortion along the reaction coordinate, leading to the three-membered ring for the bridged (nonvertical) mechanism. All nine structures (four with S, four with Se, and one with Te) had the diaxial relationship between M and the variable leaving group, and none exhibited angle distortions. As seen in Tables 4, 7, and 9, the M-C-C angles (towards the leaving group) are close to or larger than 109.5° in almost all cases (for molecules that exist in two crystallographic forms, the angles are averaged). For the four sulfur compounds (**4f, 4g, 4h, 7m**) the respective S-C-C angles are 109.77, 112.16, 109.95, and 110.47°. For the four selenium compounds (**4i, 4j, 4k, 7k**) the respective Se-C-C angles are 109.43, 109.5, 106.54, and 109.2. For the single tellurium compound (**4l**), the Te-C-C angle is 109.15°. Except for **4g** and **4k**, all these values are normal, and only **4k** shows any tendency to be smaller (vide infra). We conclude that the angles do not indicate movement along the reaction coordinate towards bridging. It also is noteworthy that the C-C-C angles within the ring at the positions of M and O substitution also show no systematic angle distortions in response to syn-axial repulsion between the substituent and hydrogens across the ring.

The absence of a structural trend is not strong evidence. It still is necessary to probe whether bond lengths reflect movement along the reaction coordinate. The data in Tables 3

and 6 show that the C–O distances increase with increasing electron demand of the leaving group for both the sulfur and the selenium systems, as best seen in Figure 5. The plots may be fitted to Equation (4) for sulfur and Equation (5) for selenium.

$$r(\mathrm{C{-}O}) = 1.484 - (4.62 \times 10^{-3})\mathrm{p}K_a \quad (4)$$

$$r(\mathrm{C{-}O}) = 1.493 - (5.33 \times 10^{-3})\mathrm{p}K_a \quad (5)$$

Both equations show good linearity (r^2 is 1.000 for S and 0.991 for Se). These equations may be compared with those for H [Eq. (6)][8] and Si [Eq. (7)].[7]

$$r(\mathrm{C{-}O}) = 1.475 - (2.90 \times 10^{-3})\mathrm{p}K_a \quad (6)$$

$$r(\mathrm{C{-}O}) = 1.502 - (5.30 \times 10^{-3})\mathrm{p}K_a \quad (7)$$

In terms of C–O bond lengthening, sulfur with a slope of -4.62 (aside from the exponent) generates a considerably stronger response than hydrogen (-2.90), but slightly weaker than silicon (-5.30). Selenium (-5.33) is comparable to silicon.

As we have only a single point for tellurium, we cannot present an analogous plot. The C–O bond length of 1.473 Å for **4l** (an acetate), however, is seen to be lengthened according to the following argument. The analogous values for the acetate leaving group were not available for S and Se, but may be calculated from Equations (4) and (5) from the known value of the pK_a for acetic acid (4.76). In this way we generated the bond length series of 1.462 (calcd), 1.467 (calcd), and 1.473 Å (obsd) for S, Se, and Te, respectively. The monotonic increase along this series is consistent with increasing σ-donor abilities of the C–S, C–Se, and C–Te bonds.

Two of the selenium structures had 2,4-nitrobenzoate as the leaving group (**4k** and **7k**). The value for **4k** fell below the plot in Figure 5, indicating an unexpectedly short bond length (1.474(2) Å). Moreover, it is marginally shorter than even the corresponding sulfur system **4h** (1.477(2) Å) (the more electron-donating Se should generate the longer bond). A possible explanation of this short C–O bond length is provided by examination of the conformation of the carboxyl group in **4k** in the crystal structure (Figure 4). The dihedral angle O-C-C(*ipso*)-C(*ortho*) is $-79.1(2)$ (Table 8), so that the carboxyl group is essentially orthogonal to the electron-deficient 2,4-dinitrobenzoate ring. In all other benzoate esters (**4f, 4g, 4h, 4j, 7k**), the carboxylate group is nearly coplanar with the aromatic ring, as the dihedral angles (Tables 5 and 8) are close to 0 or 180°. The less effective π overlap between the orthogonal groups should make the ester oxygen in **4k** less electron demanding than in the other 2,4-dinitrobenzoates (**7k** and **4h**) and hence cause less bond lengthening. Since **4k** is structurally distinct from all other systems, we excluded it from Figure 1. This conformational difference also is probably responsible for the uniquely smaller M-C-C bond angle mentioned above.

Conclusions

Kinetic measurements on systems in which sulfur (**4d**) or selenium (**4e**) is constrained to the antiperiplanar relationship to a leaving group provide respective rate enhancements of 10^5 and 10^6 over the analogous system in which the β functionality is replaced by hydrogen. These values compare with considerably higher enhancements for structurally analogous silicon (10^{12}) and germanium (10^{13}) systems.[9, 13] The Group 14 atoms, however, are much less electronegative than the Group 16 atoms and, hence, are more electron donating. The large rate enhancements are maintained in the unbiased trans systems (**6d** and **6e**), despite an admixture of the less reactive diequatorial conformer.

These rate enhancements are consistent with either backside displacement in the bridging or nonvertical mechanism [Eqs. (1) and (2a)] or with carbocation stabilization in the nonbridging or vertical mechanism [Eqs. (2b) and (3)]. The nonbridging mechanism, in which the carbocation is stabilized by hyperconjugation, has been proved in the analogous cases of Si, Ge, and Sn participation. The presence of lone pairs on the participating atom clearly provides no kinetic advantage, as the S and Se systems are much slower than the Group 14 systems. The vertical mechanism also can explain the large rate enhancement even with the diequatorial admixed, as hyperconjugation is still significant for the 60° geometry, whereas the nonvertical mechanism is entirely excluded in this geometry.

Products from both sulfur and selenium systems are consistent with either vertical or nonvertical mechanisms, although observation of two isomers in the reaction of the selenium substrate suggests strong carbocationic character in the product-forming step.

Further evidence for the vertical mechanism comes from the variable oxygen probe. The crystal structures of four sulfur systems generated a plot (Figure 5) in which the lengthening of the C–O bond is seen to depend upon the basicity of the leaving group. This lengthening expresses movement along the reaction coordinate towards the carbocation. Moreover, bond lengthening is not accompanied by angle distortions towards the three-membered ring of Equation (1) and (2a). The X-ray data thus support movement along the reaction coordinate towards the nonbridging pathway in which positive charge is stabilized vertically by hyperconjugation. The case is even stronger from the analogous plot for selenium (Figure 5). The slopes of these plots provide a measure of the sensitivity of the lengthening process to leaving group basicity. The slope for sulfur [Eq. (4)] is considerably larger than that for hydrogen [Eq. (6)] but less than that for silicon [Eq. (7)], whereas that for selenium [Eq. (5)] is comparable to that for silicon. A single structure with tellurium at the β-position has a C–O bond length that is longer than its sulfur and selenium analogues, indicating that σ donation is even stronger from the C–Te bond.

The variable oxygen probe confirms the presence of strong σ donation from the C–S and C–Se bonds in the ground state, without angular distortion, consistent with movement along the reaction coordinate for the vertical mechanism. These structural measurements are consistent with the conclusions

  0947-6539/02/0812-2806 $ 17.50+.50/0 *Chem. Eur. J.* **2002**, *8*, No. 12

from the kinetic measurements. Although the case for vertical participation by selenium is strong, the case for sulfur is less compelling, as kinetics and products are equally consistent with nonvertical participation and the sulfur slope in Figure 5 is lower.

Experimental Section

***r*-5-*tert*-Butyl-*c*-2-(phenylthio)cyclohexan-*t*-ol (4a)**: A solution of thiophenol (1.71 g, 15.5 mmol) in MeOH (50 mL) was treated with NaOH (0.6 g, 15 mmol). After the MeOH had dissolved, the solution was treated with *trans*-5-*tert*-butylcyclohexene oxide (2 g, 0.013 mmol). The resulting solution was heated to reflux for 90 min, and the excess MeOH was removed under vacuum. The residue was extracted with diethyl ether (50 mL), washed with H_2O (3×50 mL), dried ($MgSO_4$), filtered, and concentrated by rotary evaporation to produce a colorless, viscous oil. Excess thiophenol was removed by passing the oil through a flash chromatography column with hexane and then diethyl ether/hexane, to give a colorless oil (3.4 g, 99%). ^{1}H NMR ($CDCl_3$): $\delta=7.40-7.37$ (m, 2H), 7.29–7.17 (m, 3H), 4.08 (m, 1H), 3.38 (m, 1H), 2.23 (s, 1H; OH), 2.19–2.05 (m, 1H), 1.86–1.27 (m, 6H), 0.87 (s, 9H); ^{13}C NMR ($CDCl_3$): $\delta=135.55$, 130.77, 128.88, 126.50, 69.66, 49.09, 40.58, 32.08, 28.98, 27.28, 25.85, 21.81; IR (KBr): $\tilde{\nu}=736$, 3293 cm^{-1}; MS calcd for $C_{16}H_{24}NaOS$ [M^++Na]: 287.1446; found: 287.1445; elemental analysis calcd (%) for $C_{16}H_{24}SO$: C 72.66, H 9.14, S 12.13; found: C 71.40, H 8.95, S 11.70.

***r*-5-*tert*-Butyl-*c*-2-(phenylselenyl)cyclohexan-*t*-ol (4b):** A solution of diphenyl diselenide (1.01 g, 3.24 mmol) in absolute EtOH (10 mL) was treated with portions of $NaBH_4$ (300 mg) until the yellow color of the diselenide had disappeared. After effervescence had subsided, the solution of the phenylselenyl anion was cooled to $-78\,^\circ$C and treated with *trans*-5-*tert*-butylcyclohexene oxide (1 g, 6.5 mmol). The solution was stirred at $-78\,^\circ$C for 15 min, warmed to reach room temperature, and stirred for a further 30 min. The mixture was diluted with H_2O (50 mL) and extracted with diethyl ether (3×20 mL). The combined extracts were washed with H_2O (2×50 mL), dried ($MgSO_4$), filtered, and concentrated by rotary evaporation to give a yellow oil (1.95 g, 96%). ^{1}H NMR ($CDCl_3$): $\delta=7.55-7.51$ (m, 2H), 7.27–7.24 (m, 3H), 4.18 (m, 1H), 3.45 (m, 1H), 2.25–2.12 (m, 2H), 1.95–1.88 (m, 1H), 1.76–1.72 (m, 1H), 1.66–1.60 (m, 1H), 1.48–1.24 (m, 2H), 0.87 (s, 9H); ^{13}C NMR ($CDCl_3$): $\delta=133.61$, 130.06, 129.01, 127.20, 70.40, 47.45, 40.64, 32.10, 29.40, 27.28, 26.62, 22.88; ^{77}Se NMR ($CDCl_3$): $\delta=345.15$; IR (thin film): $\tilde{\nu}=3351$ cm^{-1}; MS calcd for $C_{16}H_{24}NaO^{80}Se$ [M^++Na]: 335.0884; found: 335.0890; elemental analysis calcd (%) for $C_{16}H_{24}SeO$: C 61.73, H 7.77; found: C 61.65, H 7.87.

***r*-4-*tert*-Butyl-*t*-2-(phenylselenyl)cyclohexan-*c*-ol (5b):** A solution of phenylselenyl anion prepared from diphenyl diselenide (0.7 g, 2.24 mmol) in EtOH (20 mL) was treated with *cis*-5-*tert*-butylcyclohexene oxide (0.44 g, 4.48 mmol). After workup (as described above), a clear oil was obtained (1.2 g, 85%). ^{1}H NMR ($CDCl_3$): $\delta=7.56$ (m, 2H), 7.28 (m, 3H), 4.08 (m, 1H), 3.57 (m, 1H), 3.15 (1H; OH), 2.1–1.8 (m, 3H), 1.8–1.0 (m, 5H), 0.9 (m, 9H); ^{13}C NMR ($CDCl_3$): $\delta=133.85$, 130.02, 129.03, 127.31, 68.97, 48.66, 43.22, 28.94, 27.36, 27.23, 26.99, 20.69.

***r*-5-*tert*-Butyl-*c*-2-(phenyltelluryl)cyclohexan-*t*-ol (4c):** A dark red solution of diphenyl ditelluride (0.66 g, 1.6 mmol) and $NaBH_4$ (177 mg) was stirred in anhydrous THF (40 mL) under an atmosphere of N_2. This solution was treated by dropwise addition of MeOH until the solution was colorless After effervescence had subsided, the solution of phenyltelluryl anion was cooled to $-78\,^\circ$C and treated with a solution of *trans*-5-*tert*-butylcyclohexene oxide (0.5 g, 3.2 mmol) in anhydrous THF (5 mL). The resulting mixture was stirred at $-78\,^\circ$C for 10 min, warmed to room temperature, and stirred for a further 60 min. The solution was diluted with H_2O (100 mL) and extracted with diethyl ether (3×20 mL). The combined extracts were washed with H_2O (4×50 mL), dried ($MgSO_4$), filtered, and concentrated by rotary evaporation to produce a red oil containing a trace of diphenyl ditelluride. Purification by flash chromatography gave a yellow oil (1.11 g, 95%), which crystallized upon standing (35–37.5 °C). ^{1}H NMR ($CDCl_3$): $\delta=7.78-7.76$ (m, 2H), 7.32–7.17 (m, 3H), 4.39 (m, 1H), 3.58 (m, 1H), 2.41–2.28 (m, 1H), 2.04–1.98 (m, 1H), 1.92 (m, 1H; OH), 1.82–1.64 (m, 3H), 1.46–1.35 (m, 1H), 1.24–1.10 (m, 1H), 0.86 (s, 9H); ^{13}C NMR ($CDCl_3$): $\delta=139.03$, 129.18, 127.83, 112.32, 72.42, 40.78, 35.58, 32.08, 30.21, 28.23, 27.28, 24.89; ^{125}Te NMR ($CDCl_3$): $\delta=569.92$; IR (KBr): $\tilde{\nu}=3311$ cm^{-1}; MS calcd for $C_{16}H_{24}NaO^{130}Te$ [M^++Na]: 385.0780; found: 385.0786; elemental analysis calcd (%) for $C_{16}H_{24}TeO$: C 53.39, H 6.72; found: C 52.81, H 6.66.

***r*-5-*tert*-Butyl-*c*-2-(phenyltelluryl)cyclohex-*t*-yl acetate (4l)**: A solution of alcohol **4c** (0.50 g, 1.39 mmol) in pyridine (2 mL) was stirred at $-5\,^\circ$C for 30 min and treated with acetyl chloride (0.22 g, 0.27 mmol). The mixture was stirred for 2 h at room temperature and then quenched with H_2O. More H_2O (20 mL) was added, and the mixture was stirred for 30 min. The mixture was extracted into diethyl ether (3×20 mL). The extracts were washed with saturated aqueous $CuSO_4$ solution (3×30 mL), H_2O (3×30 mL), saturated aqueous $NaHCO_3$ solution (3×30 mL), and H_2O (3×30 mL), dried ($MgSO_4$), filtered, and concentrated by rotary evaporation to give a yellow oil (0.48 mg, 86%), which crystallized upon standing to give yellow rectangular blocks, m.p. 55 – 57 °C. ^{1}H NMR ($CDCl_3$): $\delta=7.82-7.78$ (m, 2H), 7.31–7.18 (m, 3H), 5.40 (m, 1H), 3.70 (m, 1H), 2.32–2.20 (m, 1H), 2.12–2.40 (m, 1H), 2.03 (s, 3H), 1.91–1.82 (m, 1H), 1.77–1.64 (m, 2H), 1.42–1.31 (m, 1H), 1.26–1.11 (m, 1H), 0.86 (s, 9H); ^{13}C NMR ($CDCl_3$): $\delta=170.16$, 138.78, 129.25, 127.87, 112.29, 75.49, 14.56, 32.09, 31.56, 29.26, 27.90, 27.23, 24.68, 21.31; ^{125}Te NMR ($CDCl_3$): $\delta=576.86$; IR (KBr): $\tilde{\nu}=3433$ cm^{-1}.

***trans*-2-(Phenylthio)cyclohexanol (6a):** A solution of thiophenol (11.2 g, 0.102 mol) in MeOH (150 mL) was treated with NaOH (4 g, 0.10 mol). After the NaOH had dissolved, the solution was treated with cyclohexene oxide (10 g, 0.102 mol). The resulting solution was heated to reflux for 90 min, and the excess MeOH was removed under vacuum. The residue was dissolved in diethyl ether (100 mL), washed with H_2O (3×100 mL), dried ($MgSO_4$), filtered, and concentrated by rotary evaporation to yield a colorless viscous oil (20.8 g, 98%). ^{1}H NMR ($CDCl_3$): $\delta=7.60-7.20$ (m, 5H), 3.40 (m, 1H), 3.14 (1H; OH), .90 (m, 1H), 2.42–0.9 (m, 8H); ^{13}C NMR ($CDCl_3$): $\delta=133.69$, 128.82, 127.66, 71.92, 56.35, 33.73, 32.59, 26.06, 24.20.

***trans*-2-(Phenylselenyl)cyclohexanol (6b):** A solution of sodium phenylselenide generated from diphenyl diselenide (3.18 g, 10.2 mmol) in absolute EtOH as described above, was cooled to $-78\,^\circ$C and then treated with cyclohexene oxide (2 g, 20.4 mmol). The resulting solution was stirred at $-78\,^\circ$C, warmed to room temperature, and stirred a further 30 min. The solution was diluted with H_2O (100 mL) and extracted with diethyl ether (3×50 mL). The combined extracts were washed with H_2O (3×100 mL), dried ($MgSO_4$), filtered, and concentrated by rotary evaporation to give an oil (4.2 g, 81%). ^{1}H NMR ($CDCl_3$): $\delta=7.65$ (2H), 7.4–7.2 (m, 3H), 3.35 (m, 1H), 3.05 (1H; OH), 2.91 (m, 1H), 2.18 (m, 2H), 1.9–1.55 (m, 2H), 1.5–1.1 (m, 4H); ^{13}C NMR ($CDCl_3$): $\delta=135.98$, 131.2, 128.88, 127.99, 72.08, 53.32, 33.79, 33.25, 26.73, 24.35; elemental analysis calcd (%) for $C_{12}H_{16}SeO$: C 56.47, H 6.32; found: C 55.88, H 6.15.

***trans*-2-(Phenyltelluryl)cyclohexanol (6c):** A solution of sodium phenyltelluride in THF generated from diphenyl ditelluride (2.3 g, 5.6 mmol) as described above was cooled to $-78\,^\circ$C and treated with a solution of cyclohexene oxide (1 g, 10 mmol) in THF (5 mL). The resulting solution was stirred at $-78\,^\circ$C for 15 min and then at room temperature for 60 min. The resulting solution was diluted with H_2O (100 mL) and extracted with diethyl ether (3×50 mL). The combined extracts were washed with H_2O (4×100 mL), dried ($MgSO_4$), filtered, and concentrated by rotary evaporation to produce a red oil, which contained a small amount of diphenyl ditelluride. The oil was purified by anhydrous flash chromatography with hexane and then diethyl ether/hexane as eluents, to give the alcohol as a yellow oil (2.8 g, 90%), which crystallized upon standing. ^{1}H NMR ($CDCl_3$): $\delta=7.84$ (m, 2H), 7.37 (m, 1H), 7.24 (m, 2H), 3.45 (m, 1H), 3.12 (m, 1H), 2.76 (1H; OH), 2.34 (m, 1H), 2.17 (m, 1H), 1.8 (m, 1H), 1.65–1.45 (m, 2H), 1.4–1.15 (m, 3H); ^{13}C NMR ($CDCl_3$): $\delta=140.84$, 129.03, 128.24, 109.48, 73.50, 39.59, 35.06, 34.16, 27.78, 24.65; IR (thin film): $\tilde{\nu}=3402$ cm^{-1}; MS calcd for $C_{16}H_{24}NaO^{130}Te$ [M^++Na]: 327.0140; found: 327.0142; elemental analysis calcd (%) for $C_{12}H_{16}TeO$: C 47.43, H 5.31, Te 41.99; found: C 47.47, H 5.31, Te 41.81.

***r*-5-*tert*-Butyl-*c*-2-(phenylthio)cyclohex-*t*-yl trifluoroacetate (4d):** A solution of the alcohol **4a** (0.42 g, 1.59 mmol) in anhydrous diethyl ether (10 mL) in the presence of pyridine (0.25 g, 3.18 mmol) was stirred at $-10\,^\circ$C under an atmosphere of N_2 and treated with trifluoroacetic anhydride (0.4 g, 1.9 mmol) in a dropwise fashion. The solution immedi-

ately produced a thick white precipitate. It was stirred for 20 min at −10 °C. The resulting mixture was diluted with H_2O (50 mL), and the diethyl ether layer was separated. The extracts were washed with saturated aqueous $CuSO_4$ (2 × 20 mL), H_2O (20 mL), saturated aqueous $NaHCO_3$ (2 × 20 mL), and H_2O again (20 mL), dried ($MgSO_4$), filtered, and concentrated by rotary evaporation to give a colorless oil (0.55 g, 96 %). ^{1}H NMR ($CDCl_3$): $\delta = 7.5$ (m, 2H), 7.4–7.25 (m, 3H), 5.31 (m, 1H), 3.57 (m, 1H), 2.4–1.9 (m, 4H), 1.8–1.4 (m, 3H), 0.92 (s, 9H); ^{13}C NMR ($CDCl_3$): $\delta =$ 131.16, 129.43, 127.82, 77.89, 44.84, 41.33, 32.06, 27.12, 26.92, 25.98, 21.44. The same general procedure was used for the trifluoroacetates described below.

***r*-5-*tert*-Butyl-*c*-2-(phenylselenyl)cyclohex-*t*-yl trifluoroacetate (4e):** The procedure for **4d** was applied to alcohol **4b** to produce a colorless oil (0.565 g, 98 %). ^{1}H NMR ($CDCl_3$): $\delta = 7.65$–7.60 (m, 2H), 7.4–7.3 (m, 3H), 5.44 (m, 1H), 3.64 (m, 1H), 2.2–2.05 (m, 2H), 2.0–1.9 (m, 2H), 1.75 (m, 1H), 1.5–1.35 (m, 2H), 0.92 (s, 9H); ^{13}C NMR ($CDCl_3$; not including CF_3CO residue): $\delta = 133.83$, 133.77, 129.33, 129.00, 127.85, 78.63, 42.90, 41.35, 32.08, 27.33, 27.14, 26.49, 22.50.

***trans*-2-(Phenylthiocyclohexyl) trifluoroacetate (6d):** The procedure for **4d** was applied to alcohol **6a** to produce a colorless oil (0.60 g, 98 %). ^{1}H NMR ($CDCl_3$): $\delta = 7.49$ (m, 2H), 7.4–7.25 (m, 3H), 4.99 (m, 1H), 3.21 (m, 1H), 2.25–2.1 (m, 2H), 1.86–1.7 (m, 2H), 1.7–1.3 (m, 4H); ^{13}C NMR ($CDCl_3$; not including CF_3CO residue): $\delta = 133.13$, 133.00, 128.93, 127.65, 79.07, 49.76, 31.44, 30.23, 30.16, 24.35, 22.99.

***trans*-2-Phenylselenylcyclohexyl trifluoroacetate (6e):** The procedure for **4d** was applied to alcohol **6b** to produce a colorless oil (0.586 g, 99 %). ^{1}H NMR ($CDCl_3$): $\delta = 7.61$ (m, 2H), 7.4–7.25 (m, 3H), 5.05 (m, 1H), 3.25 (m, 1H), 2.32–2.14 (m, 2H), 1.8–1.25 (6H, m); ^{13}C NMR ($CDCl_3$; not including CF_3CO residue): $\delta =$ 135.53, 129.05, 128.13, 79.34, 44.87, 32.00, 30.59, 25.14, 23.07.

Product analyses of the solvolysis of *r*-5-*tert*-butyl-*c*-2-(phenylthio)cyclohex-*t*-yl trifluoroacetate: A solution of the trifluoroacetate **4d** (180 mg, 5 mmol) in 97 % (w/w) aqueous trifluoroethanol (TFE, 15 mL) was left at room temperature for 48 h. The solution was then diluted with H_2O (30 mL) and extracted with diethyl ether. The extracts were evaporated down to an oil (140 mg), which was shown by NMR spectroscopy to be essentially pure *r*-5-*tert*-butyl-*c*-2-(phenylthio) cyclohexan-*t*-ol (100 % recovery).

Product analysis of the solvolysis of *r*-5-*tert*-butyl-*c*-2-(phenylselenyl)cyclohex-*t*-yl trifluoroacetate: A solution of the trifluoroacetate **4e** (0.12 g, 3 mmol) was dissolved in 97 % aqueous TFE and left at room temperature overnight. The solution was then diluted with H_2O (30 mL) and extracted with diethyl ether. The extracts were evaporated down to an oil (95 mg), which was shown by NMR spectroscopy to consist of an approximate 1/1.2 mixture of *r*-5-*tert*-butyl-*c*-2-(phenylselenyl)cyclohexan-*t*-ol and *r*-4-*tert*-butyl-*t*-2-(phenylselenyl)cyclohexan-*c*-ol.

Product analysis of the solvolysis of *r*-5-*tert*-butyl-*c*-2-(phenylselenyl)cyclohex-*t*-yl trifluoroacetate in the presence of excess cyclohexene: A solution of the trifluoroacetate **4e** (130 mg, 0.32 mmol) and cyclohexene (78 mg, 3 equiv) in 97 % aqueous TFE was left at room temperature for 24 h. The solution was then diluted with H_2O (30 mL) and extracted with diethyl ether. The extracts were evaporated down to produce a residue (110 mg), which was shown by NMR spectroscopy to be an approximate 1/1 mixture of 4-*tert*-butylcyclohexene and *trans*-2-(phenylselenyl)cyclohexanol.

***r*-5-*tert*-Butyl-*c*-2-(phenylthio)cyclohex-*t*-yl 4-nitrobenzoate (4f):** A solution of the alcohol **4a** (220 mg, 0.83 mmol) was stirred in pyridine (2 mL) for 30 min and treated with 4-nitrobenzoyl chloride (0.17 g, 0.91 mmol). The mixture was stirred for 3 h at room temperature and then quenched with H_2O. More H_2O (20 mL) was added, and the mixture was stirred for 30 min. The mixture was extracted with diethyl ether (3 × 20 mL), and the combined extracts were washed with saturated aqueous $CuSO_4$ solution (3 × 30 mL), H_2O (3 × 30 mL), saturated aqueous $NaHCO_3$ solution (3 × 30 mL), and H_2O (3 × 30 mL), dried ($MgSO_4$), filtered, and concentrated by rotary evaporation to give a yellow solid (0.31 mg, 90 %), which was recrystallized from petroleum ether to give yellow needles, m.p. 87–89 °C. ^{1}H NMR ($CDCl_3$): $\delta = 8.31$ (d, $J = 8.7$ Hz, 2H), 8.19 (d, $J = 9.0$ Hz, 2H), 7.52–7.48 (m, 2H), 7.40–7.22 (m, 3H), 5.40 (m, 1H), 3.65 (m, 1H), 2.2–1.40 (m, 6H), 0.91 (s, 9H); ^{13}C NMR ($CDCl_3$): $\delta = 163.68$, 150.50, 135.89, 134.81, 130.72, 130.64, 129.10, 126.90, 123.59, 74.43, 45.99, 41.98, 32.24, 27.30, 27.11, 26.43, 21.65; IR (KBr): $\tilde{\nu} = 713$, 1531, 1718 cm^{-1}.

***r*-5-*tert*-Butyl-*c*-2-(phenylthio)cyclohex-*t*-yl 3,5-dinitrobenzoate (4g):** A solution of alcohol **4a** (50 mg, 0.189 mmol) was stirred in pyridine (2 mL) for 30 min and treated with 3,5-dinitrobenzoyl chloride (0.065 g, 0.28 mmol). The mixture was stirred overnight at room temperature and then quenched with H_2O. More H_2O (20 mL) was added, and the mixture was stirred for 30 min. The mixture was extracted with diethyl ether (3 × 20 mL), and the combined extracts were washed with saturated aqueous $CuSO_4$ solution (3 × 30 mL), H_2O (3 × 30 mL), saturated aqueous $NaHCO_3$ solution (3 × 30 mL), and H_2O (3 × 30 mL), dried ($MgSO_4$), filtered, and concentrated by rotary evaporation to give a yellow solid (55.3 mg, 63.7 %), which was recrystallized from MeOH to give yellow needles, m.p. 194–195 °C. ^{1}H NMR ($CDCl_3$): $\delta = 9.27$ (t, $J = 2.1$ Hz, 1H), 9.13 (d, $J = 2.4$ Hz, 2H), 7.52–7.49 (m, 2H), 7.37–7.22 (m, 3H), 5.45 (m, 1H), 3.67 (m, 1H), 2.2–1.99 (m, 4H), 1.82–1.73 (m, 1H), 1.60–1.48 (m, 2H), 0.93 (s, 9H); ^{13}C NMR ($CDCl_3$): $\delta = 161.58$, 148.66, 134.54, 134.18, 130.99, 129.29, 129.15, 127.14, 122.35, 75.94, 46.12, 42.03, 32.26, 27.29, 27.17, 26.41, 21.64; IR (KBr): $\tilde{\nu} = 718$, 1541, 1720 cm^{-1}.

***r*-5-*tert*-Butyl-*c*-2-(phenylthio)cyclohex-*t*-yl 2,4-dinitrobenzoate (4h)**: A solution of the alcohol **4a** (54 mg, 0.20 mmol) was stirred in pyridine (2 mL) for 30 min and then treated with 2,4-dinitrobenzoyl chloride (0.071 g, 0.30 mmol). The mixture was stirred overnight at room temperature and then quenched with H_2O. More H_2O (20 mL) was added, and the mixture was stirred for 30 min. The mixture was extracted into diethyl ether (3 × 20 mL), and the combined extracts were washed with saturated aqueous $CuSO_4$ solution (3 × 30 mL), H_2O (3 × 30 mL), saturated aqueous $NaHCO_3$ solution (3 × 30 mL), and H_2O (3 × 30 mL), dried ($MgSO_4$), filtered, and concentrated by rotary evaporation to give yellow solid (61.2 mg, 65.2 %), which was recrystallized from MeOH to give yellow rectangular blocks, m.p. 103–105 °C. ^{1}H NMR ($CDCl_3$): $\delta = 8.78$ (d, $J =$ 2.1 Hz, 1H), 8.56 (dd, $J = 8.55$ Hz, $J = 2.25$ Hz, 1H), 7.99 (d, $J = 8.4$ Hz, 1H), 7.54–7.52 (m, 2H), 7.40–7.26 (m, 3H), 5.45 (m, 1H), 3.71 (m, 1H), 2.03–1.94 (m, 4H), 1.72–1.64 (m, 1H), 1.53–1.30 (m, 2H), 0.93 (s, 9H); ^{13}C NMR ($CDCl_3$): $\delta = 162.77$, 148.92, 148.26, 134.65, 132.67, 131.49, 130.59, 129.08, 127.26, 126.88, 119.42, 76.57, 45.44, 41.47, 32.13, 32.13, 27.16, 26.89, 26.11, 21.47; IR (KBr): $\tilde{\nu} = 730$, 1546, 1714 cm^{-1}.

***r*-5-*tert*-Butyl-*c*-2-(phenylselenyl)cyclohex-*t*-yl 4-nitrophenoxide (4i):** A suspension of NaH (0.1 g 60 %) in anhydrous THF (10 mL) was treated with a solution of the alcohol **4b** (49.8 mg, 0.159 mmol) in anhydrous THF (10 mL). The resulting solution was stirred at room temperature for 1 h. The resulting mixture was chilled in ice, a solution of 4-fluoronitrobenzene (0.025 mL, 0.235 mmol) in anhydrous THF (5 mL) was added, and the reaction was stirred for 18 h. Excess NaH was destroyed by the careful addition of H_2O, and the resulting mixture was extracted with diethyl ether (3 × 20 mL). The combined extracts were washed with H_2O (3 × 30 mL), dried ($MgSO_4$), filtered, and concentrated by rotary evaporation to give a white solid (60.6 mg, 87.6 %), which was recrystallized from MeOH to give white rectangular plates, m.p. 69–71 °C. ^{1}H NMR ($CDCl_3$): $\delta = 8.02$ (d, $J =$ 9.3 Hz, 2H), 7.66–7.63 (m, 2H), 7.43–7.31 (m, 3H), 6.56 (d, $J = 9.3$ Hz, 2H), 4.59 (m, 1H), 3.67 (m, 1H), 2.31–2.20 (m, 1H), 2.03–1.95 (m, 2H), 1.92–1.82 (m, 1H), 1.71–1.63 (m, 1H), 1.52–1.11 (m, 2H), 0.88 (s, 9H); ^{13}C NMR ($CDCl_3$): $\delta = 162.48$, 141.10, 135.31, 129.34, 129.13, 128.34, 125.87, 115.04, 74.96, 44.90, 43.10, 32.30, 27.98, 27.32, 26.27, 21.34; ^{77}Se NMR ($CDCl_3$): $\delta = 364.89$; IR (KBr): $\tilde{\nu} = 1260$, 1591 cm^{-1}.

***r*-5-*tert*-Butyl-*c*-2-(phenylselenyl)cyclohex-*t*-yl 4-nitrobenzoate (4j)**: A solution of the alcohol (**4b**, 100 mg, 0.38 mmol) was stirred in pyridine (2 mL) for 30 min and treated with 4-nitrobenzoyl chloride (0.077 g, 0.42 mmol). The mixture was stirred for 3 h at room temperature and quenched with H_2O. More H_2O (20 mL) was added, and the mixture was stirred for 30 min. The mixture was extracted with diethyl ether (3 × 20 mL), and the combined extracts were washed with saturated aqueous $CuSO_4$ solution (3 × 30 mL), H_2O (3 × 30 mL), saturated aqueous $NaHCO_3$ solution (3 × 30 mL), and H_2O (3 × 30 mL), dried ($MgSO_4$), and concentrated by rotary evaporation to give a yellow solid (69.5 mg, 78.2 %), which was recrystallized from petroleum ether to give yellow needles, m.p. 81–83 °C. ^{1}H NMR ($CDCl_3$): $\delta = 8.29$ (d, $J = 9.0$ Hz, 2H), 8.18 (d, $J = 8.7$ Hz, 2H), 7.64–7.61 (m, 2H), 7.31–7.28 (m, 3H), 5.52 (m, 1H), 3.72 (m, 1H), 2.28–2.14 (m, 1H), 2.14–1.90 (m, 2H), 1.82–7–1.71 (m, 1H), 1.57–1.34 (m, 1H), 1.30–1.20 (m, 1H), 0.91 (s, 9H); ^{13}C NMR ($CDCl_3$): $\delta = 163.57$, 150.42, 135.90, 133.47, 131.64, 130.56, 129.17, 127.48, 123.50, 75.22, 43.64, 41.97, 32.18, 27.78,

  0947-6539/02/0812-2808 $ 17.50+.50/0 *Chem. Eur. J.* **2002**, *8*, No. 12

27.24, 26.98, 22.67; ^{77}Se NMR ($CDCl_3$): $\delta = 352.42$; IR (KBr): $\tilde{\nu} = 1529$, 1716 cm^{-1}.

***r*-5-*tert*-Butyl-*c*-2-(phenylselenyl)cyclohex-*t*-yl 2,4-dinitrobenzoate (4k):** A solution of the alcohol **4b** (54.7 mg, 0.175 mmol) was stirred in pyridine (2 mL) for 30 min and treated with 2,4-dinitrobenzoyl chloride (0.06 g, 0.26 mmol). The mixture was stirred overnight at room temperature and then quenched with H_2O. More H_2O (20 mL) was added, and the mixture was stirred for 30 min. The mixture was extracted with diethyl ether (3 × 20 mL), and the combined extracts were washed with saturated aqueous $CuSO_4$ solution (3 × 30 mL), H_2O (3 × 30 mL), saturated aqueous $NaHCO_3$ solution (3 × 30 mL), and H_2O (3 × 30 mL), dried ($MgSO_4$), filtered, and concentrated by rotary evaporation to give a yellow solid (69.5 mg, 78.2 %), which was recrystallized from pentane to give yellow rectangular blocks, m.p. 111 – 113 °C, and additionally from MeOH, m.p. 113.5 – 115.5 °C. ^{1}H NMR ($CDCl_3$): $\delta = 8.70$ (d, $J = 2.1$ Hz, 1H), 8.51 (dd, $J = 2.1$ Hz, $J =$ 8.4 Hz, 1H), 7.96 (d, $J = 8.4$ Hz, 1H), 7.64 – 7.60 (m, 2H), 7.33 – 7.29 (m, 3H), 5.40 (m, 1H), 3.81 (m, 1H), 2.28 – 2.14 (m, 1H), 2.08 – 1.92 (m, 2H), 1.83 – 1.62 (m, 2H), 1.45 – 1.15 (m, 2H), 0.86 (s, 9H); ^{13}C NMR ($CDCl_3$): $\delta =$ 162.62, 148.95, 148.43, 133.52, 132.50, 131.64, 129.65, 129.22, 127.58, 127.14, 119.33, 76.13, 44.24, 42.87, 32.28, 28.35, 27.27, 26.19, 21.48; ^{77}Se NMR ($CDCl_3$): $\delta = 361.47$; IR (KBr): $\tilde{\nu} = 1543$, 1735 cm^{-1}.

***r*-5-Methyl-*c*-2-(phenylthio)cyclohexan-*t*-ol (7a):** A solution of NaOH (0.2 g, 5.0 mmol) in MeOH (20 mL) was stirred at 0 °C under an atmosphere of N_2. Thiophenol (0.49 g, 4.46 mmol) was added to the solution, and the solution was stirred until the NaOH had dissolved. *trans*-5-Methylcyclohexene oxide (0.5 g, 4.46 mmol) was added, and the mixture was stirred for 20 min. The reaction was then diluted with H_2O (20 mL) and extracted with petroleum ether (30 mL, b.p. 40 – 60 °C). The organic layer was washed with H_2O (2 × 30 mL), dried ($MgSO_4$), filtered, and concentrated by rotary evaporation to give a pale yellow oil (0.77 g, 78 %). ^{1}H NMR ($CDCl_3$): $\delta = 7.42 – 7.40$ (m, 2H), 7.35 – 7.20 (m, 3H), 3.79 (m, 1H), 3.05 (m, 1H), 2.45 (s, 1H; OH), 2.10 – 1.92 (m, 2H), 1.90 – 1.79 (m, 1H), 1.75 – 1.60 (m, 1H), 1.60 – 1.42 (m, 2H), 1.42 – 1.37 (m, 1H), 0.9 (d, $J =$ 6.9 Hz, 3H); ^{13}C NMR ($CDCl_3$): $\delta = 134.07$, 132.24, 128.87, 127.10, 68.58, 53.51, 38.05, 30.56, 26.97, 26.55, 20.01.

***r*-5-Methyl-*c*-2-(phenylselenyl)cyclohexan-*t*-ol (7b):** Diphenyl diselenide (0.7 g, 2.24 mmol) was stirred in EtOH (7 mL) under an atmosphere of N_2, and $NaBH_4$ (280 mg) was added in portions until the solution was colorless. The solution was then cooled to 0 °C, and *trans*-5-methylcyclohexene oxide (0.5 g, 4.46 mmol) was added. The mixture was stirred for 15 min and diluted with H_2O (25 mL). The mixture then was extracted with diethyl ether (30 mL). The organic layer was washed with H_2O (2 × 30 mL), dried ($MgSO_4$), filtered, and concentrated by rotary evaporation to give a pale yellow oil (0.86 g, 72 %). ^{1}H NMR ($CDCl_3$): $\delta = 7.61 – 7.57$ (m, 2H), 7.36 – 7.61 (m, 3H), 3.82 (m, 1H), 3.17 (m, 1H), 2.60 (s, 1H; OH), 2.18 – 2.02 (m, 1H), 2.02 – 1.90(m, 1H), 1.90 – 1.70 (m, 2H), 1.63 – 1.45 (m, 2H), 1.40 – 1.23 (m, 1H), 0.87 (3H, d, $J = 6.9$ Hz); ^{13}C NMR ($CDCl_3$): $\delta = 134.82$, 128.95, 128.25, 127.62, 68.89, 50.96, 38.28, 31.40, 27.24, 27.10, 19.92; ^{77}Se NMR ($CDCl_3$): $\delta = 340.24$; IR (thin film): $\tilde{\nu} = 3392$ cm^{-1}; MS calcd for $C_{16}H_{24}NaO^{80}Se$ [M^++Na]: 293.0414; found: 293.0417.

Table 10. Crystallographic parameters for compounds **7m, 4f, 4g, 4h**, and **4i**.

	7m	**4f**	**4g**	**4h**	**4i**
formula	$C_{19}H_{21}NO_3S$	$C_{23}H_{27}NO_4S$	$C_{23}H_{26}N_2O_6S$	$C_{23}H_{26}N_2O_6S$	$C_{22}H_{27}NO_3Se$
M_r	343.43	413.52	458.52	458.52	432.41
T [K]	130.0(1)	130.0(1)	293	200.0(1)	130.0(1)
radiation	$Mo_{K\alpha}$	$Cu_{K\alpha}$	$Cu_{K\alpha}$	$Cu_{K\alpha}$	$Cu_{K\alpha}$
λ [Å]	0.71069	1.54180	1.5418	1.5418	1.5418
crystal system	triclinic	triclinic	monoclinic	triclinic	triclinic
space group	$P\bar{1}$	$P\bar{1}$	$P2_1/n$	$P\bar{1}$	$P\bar{1}$
a [Å]	10.287(5)	6.5430(10)	15.4690(15)	13.2970(15)	6.4497(4)
b [Å]	12.970(3)	15.864(2)	7.2649(5)	13.332(5)	17.1293(10)
c [Å]	13.458(4)	20.822(3)	20.382(2)	14.182(3)	20.677(3)
α [°]	82.22(2)	81.96(2)		86.61(2)	67.80(1)
β [°]	75.81(3)	86.11(2)	92.946(8)	71.850(13)	85.79(1)
γ [°]	79.47(3)	85.850(10)			72.53(2)
V [Å^3]	1703.8(10)	2130.8(5)	2287.5(4)	2277.2(9)	2095.6(4)
Z	4	4	4	4	4
ρ_{calcd} [mg m^{-3}]	1.339	1.289	1.331	1.337	1.650
μ [mm^{-1}]	0.207	1.585	1.613	1.620	2.753
$F(000)$	728	880	968	968	896
crystal size [mm]	0.6 × 0.4 × 0.15	0.6 × 0.1 × 0.04	0.6 × 0.2 × 0.15	0.3 × 0.3 × 0.2	0.4 × 0.15 × 0.07
θ range [°]	2.07 – 25.00	2.15 – 69.99	3.50 – 69.97	3.48 – 70.01	2.31 – 74.91
index range	$0 <= h <= 12$	$0 <= h <= 7$	$0 <= h <= 18$	$-15 <= h <= 16$	$-8 <= h <= 0$
	$-15 <= k <= 15$	$-19 <= k <= 19$	$0 <= k <= 8$	$-15 <= k <= 16$	$-21 <= k <= 21$
	$-15 <= l <= 16$	$25 <= l <= 25$	$-24 <= l <= 24$	$-17 <= l <= 17$	$-25 <= l <= 25$
absorption method[a]	NA	analytical	analytical	NA	analytical
max/min transmission	NA	0.93/0.61	0.80/0.54	NA	0.83/0.44
reflns collected	6361	8802	4489	9141	9308
independent reflns	5994	8043	4322	8617	8572
R(int)	0.0102	0.0294	0.0258	0.0142	0.0599
observed reflns [$I > 2\sigma(I)$]	5448	6675	3213	7301	7160
data/restraints/parameters	5994/0/602	8043/0/740	4322/0/290	8617/0/786	8572/0/488
GOF on F^2	1.034	1.013	1.028	1.059	1.012
final R indices [$I > 2\sigma(I)$]	$R1 = 0.0427$	$R1 = 0.0384$	$R1 = 0.0527$	$R1 = 0.0425$	$R1 = 0.0411$
	$wR2 = 0.1108$	$wR2 = 0.0937$	$wR2 = 0.1411$	$wR2 = 0.1141$	$wR2 = 0.1034$
R indices (all data)	$R1 = 0.0469$	$R1 = 0.0498$	$R1 = 0.0710$	$R1 = 0.0504$	$R1 = 0.0519$
	$wR2 = 0.1141$	$wR2 = 0.1005$	$wR2 = 0.1614$	$wR2 = 0.1203$	$wR2 = 0.1106$
weighting scheme[b]	$A = 0.0569$	$A = 0.0531$	$A = 0.0817$	$A = 0.0619$	$A = 0.0641$
	$B = 1.6032$	$B = 0.7365$	$B = 0.76$	$B = 0.82$	$B = 1.42$
extinction coefficient	0.0045(9)	0.00094(14)	0.0010(3)	0.00083(16)	0.00018(10)
largest diff. peak/hole [e Å^{-3}]	1.36/ – 0.48	0.29/ – 0.23	0.28/ – 0.27	0.30/ – 0.44	1.02/ – 0.81

[a] NA = not applicable. [b] $w = 1/[\sigma^2(F_o^2) + (AP)^2 + BP]$; in which $P = (F_o^2 + 2F_c^2)/3$.

Table 11. Crystallographic parameters for compounds **4j, 7k, 4l**, and **4k**.

	4j	**7k**	**4l**	**4k**
formula	$C_{23}H_{27}NO_4Se$	$C_{20}H_{20}N_2O_6Se$	$C_{18}H_{26}O_2Te$	$C_{23}H_{26}N_2O_6Se$
M_r	460.42	463.34	401.99	505.43
T [K]	130.0(1)	130.0(1)	173(2)	130.0(1)
radiation	$Mo_{K\alpha}$	$Mo_{K\alpha}$	$Mo_{K\alpha}$	$Cu_{K\alpha}$
λ [Å]	0.71069	0.71069	0.71069	1.5418
crystal system	triclinic	triclinic	monoclinic	triclinic
space group	$P\bar{1}$	$P\bar{1}$	$P2_1/c$	$P\bar{1}$
a [Å]	6.5152(18)	7.560(3)	12.5353(3)	8.1390(13)
b [Å]	15.991(4)	11.082(4)	17.1247(4)	11.1470(11)
c [Å]	20.957(4)	12.678(5)	8.4189(2)	12.652(2)
α [°]	82.446(16))	108.04(2)		86.230(13)
β [°]	86.74(2)	101.82(2)	101.433(1)	85.820(13)
γ [°]	82.370(8)	85.58(2)	99.45(2)	85.31(2)
V [Å^3]	2155.6(8)	958.5(6)	1771.37(7)	1138.9(3)
Z	4	2	4	2
ρ_{calcd} [mg m^{-3}]	1.419	1.605	1.507	1.474
μ [mm^{-1}]	1.770	2.000	1.682	2.591
$F(000)$	952	472	808	520
crystal size [mm]	0.7 × 0.14 × 0.10	0.4 × 0.3 × 0.1	0.4 × 0.4 × 0.15	0.7 × 0.25 × 0.07
θ range [°]	2.21 – 26.98	2.14 – 25.01	2.04 – 27.43	3.51 – 74.96
index range	$-1 <= h <= 8$	$-8 <= h <= 8$	$-16 <= h <= 16$	$-10 <= h <= 8$
	$-20 <= k <= 20$	$-13 <= k <= 13$	$-22 <= k <= 22$	$-13 <= k <= 13$
	$-26 <= l <= 26$	$-15 <= l <= 15$	$-10 <= l <= 10$	$-15 <= l <= 15$
absorption method	analytical	analytical	semiempirical	
max/min transmission	0.86/0.73	0.79/0.50	0.69/0.53	0.82/0.34
reflns collected	11927	7226	17681	5497
independent reflns	9411	3342	4040	4668
R(int)	0.0230	0.0219	0.0246	0.0272
observed reflns [$I > 2\sigma(I)$]	6827	3005	3361	4453
data/restraints/parameters	9411/0/740	3342/0/343	4040/0/295	4668/0/368
GOF on F^2	1.023	1.113	0.927	1.048
final R indices [$I > 2\sigma(I)$]	$R1 = 0.0388$	$R1 = 0.0425$	$R1 = 0.0191$	$R1 = 0.0284$
	$wR2 = 0.0759$	$wR2 = 0.0977$	$wR2 = 0.0449$	$wR2 = 0.0725$
R indices (all data)	$R1 = 0.0697$	$R1 = 0.0492$	$R1 = 0.0247$	$R1 = 10.0299$
	$R2 = 0.0858$	$wR2 = 0.1013$	$wR2 = 0.0461$	$wR2 = 0.0735$
weighting scheme[a]	$A = 0.0411$	$A = 0.0381$	$A = 0.0268$	$A = 0.0374$
	$B = 0.2545$	$B = 2.3758$P	$B = 0.0$	$B = 0.76$
extinction coefficient	0.0016(3))	0	0	0.0026(2)
largest diff. peak/hole [e Å^{-3}]	0.65/ − 0.48	1.45/ − 0.754	0.54/ − 0.50	0.59/ − 0.47

[a] $w = 1/[\sigma^2(F_o^2) + (AP)^2 + BP]$; in which $P = (F_o^2 + 2F_c^2)/3$.

***r*-5-Methyl-*c*-2-(phenylselenyl)cyclohex-*t*-yl 2,4-dinitrobenzoate (7k):** A solution of alcohol **7b** (55 mg, 0.204 mmol) was stirred in pyridine (2 mL) at 0 °C under N_2 for 30 min and treated with 2,4-dinitrobenzoyl chloride (0.07 g, 0.30 mmol). The mixture was stirred overnight at room temperature and then quenched with H_2O. More H_2O (20 mL) was added, and the mixture was stirred for 30 min. The mixture was extracted with diethyl ether (3 × 20 mL). The combined extracts were washed with saturated aqueous $CuSO_4$ solution (3 × 30 mL), H_2O (3 × 30 mL), saturated aqueous $NaHCO_3$ solution (3 × 30 mL), and H_2O (3 × 30 mL), dried ($MgSO_4$), filtered, and concentrated by rotary evaporation to produce a yellow solid (64.5 mg, 68 %), which was recrystallized from MeOH to give yellow blocks, m.p. 80 – 81 °C. ^{1}H NMR ($CDCl_3$): $\delta = 8.75$ (s, $J = 2.1$ Hz, 1H), 8.50 (dd, $J = 2.25$ Hz, $J = 8.25$ Hz, 1H), 7.92 (d, $J = 8.4$ Hz, 1H), 7.62 – 7.58 (m, 2H), 7.32 – 7.26 (m, 3H), 5.43 (m, 1H), 3.64 (m, 1H), 2.12 – 1.54 (m, 6H), 1.38 – 1.42 (m, 1H), 0.95 (d, $J = 6.6$ Hz, 3H); ^{13}C NMR ($CDCl_3$): $\delta = 162.78$, 148.88, 133.73, 132.92, 131.46, 129.22, 127.62, 127.31, 119.44, 76.75, 43.32, 34.42, 30.42, 27.32, 27.06, 21.43; ^{77}Se NMR ($CDCl_3$): $\delta = 359.45$; IR (KBr): $\tilde{\nu} = 1546$, 1719 cm^{-1}.

***r*-5-Methyl-*c*-2-(phenylthio)cyclohex-*t*-yl 4-Nitrophenoxide (7m):** A suspension of NaH (0.1 g 60 %) in anhydrous THF (10 mL) was treated with a solution of the alcohol **7a** (51 mg, 0.19 mmol) in anhydrous THF (10 mL). The resulting solution was stirred at room temperature for 1 h. The resulting mixture was chilled in ice. A solution of 4-fluoronitrobenzene (0.024 mL, 0.228 mmol) in anhydrous THF (5 mL) was added, and the reaction was stirred for 18 h. Excess NaH was destroyed by the careful addition of H_2O, and the resulting mixture was extracted with diethyl ether (3 × 20 mL). The combined extracts were washed with H_2O (3 × 30 mL), dried ($MgSO_4$), filtered, and concentrated by rotary evaporation to give a yellow solid (53.5 mg, 82 %), which was recrystallized from pentane to give large dark yellow blocks, m.p. 62 – 63 °C. ^{1}H NMR ($CDCl_3$): $\delta = 8.07$ (d, $J = 9.3$ Hz, 2H), 7.50 – 7.46 (m, 2H), 7.39 – 7.30 (m, 3H), 6.65 (d, $J = 9.3$ Hz, 2H), 4.56 (m, 1H), 3.48 (m, 1H), 2.19 – 2.07 (m, 1H), 1.95 – 1.80 (m, 4H), 1.64 – 1.54 (m, 1H), 1.44 – 1.30 (m, 1H), 0.96 (d, $J = 5.7$ Hz, 3H); ^{13}C NMR ($CDCl_3$): $\delta = 162.44$, 141.12, 134.31, 132.68, 129.14, 127.74, 125.85, 114.96, 75.36, 46.75, 33.61, 29.31, 26.48, 26.15, 21.86; IR (KBr): $\tilde{\nu} = 752$, 1250, 1590 cm^{-1}.

Crystallography: Diffraction data were recorded on an Enraf Nonius CAD4f diffractometer operating in the $\theta/2\theta$ scan mode at low temperature: 130 K for **4f**, **4i**, **4j**, **4k**, **7k**, and **7m**, 200 K for **4h**, and 173 K for **4l**. Diffraction data for **4l** were recorded on a Siemens SMART diffractometer at 173 K (see Tables 10 and 11 for details of the crystallographic data). The crystals were flash-cooled by means of an Oxford Cryostream cooling device. Because **4g** underwent a destructive phase change upon cooling, even when cooled slowly, data were collected at room temperature. Unit cell dimensions were corrected for any θ zero errors by centering reflections at both positive and negative θ angles. The data were corrected for Lorentz and polarization effects[14] and for absorption (SHELX-76).[15] Structures were solved by direct methods (SHELXS-86)[16] and were refined on F^2 (SHELXL-97).[17] Thermal ellipsoid plots were drawn using the program ZORTEP.[18]CCDC-180500 to CCDC-180508 contain the supplementary crystallographic data for this paper. These data can be obtained free of charge via www.ccdc.cam.ac.uk/conts/retrieving.html (or from the Cambridge Crystallographic Data Centre, 12 Union Road, Cambridge CB2 1EZ, UK; fax: (+44) 1223-336-033; or e-mail: deposit@ccdc.cam.ac.uk).

Kinetic methods: Rates were determined conductometrically with a YSI Model 32 conductance meter. The conductance cell had a 40 mL capacity and Pt electrodes. The temperature was kept constant with a Precision H8 heating bath. Usually the concentration of the substrate was approximately 10^{-4} M.

Acknowledgements

The authors thank the National Science Foundation (Grant No. CHE-0091162) and the Australian Research Council for support of this research.

[1] K. D. Gundermann, *Angew. Chem.* **1963**, *75*, 1194; *Angew. Chem. Int. Ed. Engl.* **1963**, *2*, 674 – 683.
[2] E. Block, *Reactions of Organosulfur Compounds*, Academic Press, New York, **1978**.
[3] J. B. Lambert, *Tetrahedron* **1990**, *46*, 2677 – 2689.

  0947-6539/02/0812-2810 $ 17.50+.50/0

[4] J. B. Lambert, Y. Zhao, R. W. Emblidge, L. A. Salvador, X. Liu, J-H. So, E. Chelius, *Acc. Chem. Res.* **1999**, *32*, 183–190.
[5] W. Hanstein, H. J. Berwin, T. G. Traylor, *J. Am. Chem. Soc.* **1970**, *92*, 829–836; T. G. Traylor, W. Hanstein, H. J. Berwin, N. A. Clinton, R. S. Brown, *J. Am. Chem. Soc.* **1971**, *93*, 5715–5725.
[6] A. J. Briggs, R. Glenn, P. G. Jones, A. J. Kirby, P. J. Ramaswama, *J. Am. Chem. Soc.* **1984**, *106*, 6200–6206.
[7] A. J. Green, J. Giordano, J. M. White, *Aust. J. Chem*. **2000**, *53*, 285–292.
[8] R. D. Amos, N. C. Hardy, P. G. Jones, A. J. Kirby, J. K. Parker, J. M Percy, M. D. Su, *J. Chem. Soc. Perkins Trans. 2* **1992**, *4*, 549–558.
[9] J. B. Lambert, G.-t. Wang, R. B. Finzel, D. H. Teramura, *J. Am. Chem. Soc.* **1987**, *109*, 7838–7845.
[10] R. J. Scarborough, Jr., A. B. Smith, W. E. Barnette, K. C. Nicolaou, *J. Org. Chem*. **1979**, *44*, 1742–1744.
[11] T. Hori, K. B. Sharpless, *J. Org. Chem.*, **1978**, *43*, 1689–1697.
[12] T. Wirth, G. Fragale, M. Spichty, *J. Am. Chem. Soc*. **1998**, *120*, 3376–3381.
[13] J. B. Lambert, G.-t. Wang, D. H. Teramura, *J. Org. Chem.* **1988**, *53*, 5422–5428.
[14] R. W. Gable, B. F. Hoskins, A. Linden, I. A. S. McDonald, R. J. Steen, Program for Processing of CAD-4 Diffractometer Data, University of Melbourne (Australia), **1994**.
[15] G. M. Sheldrick, SHELX-76: Program for Crystal Structure Determination, Cambridge (England) **1976**.
[16] SHELXS-86: G. M. Sheldrick in *Crystallographic Computing 3* (Eds.: G. M. Sheldrick, C. Kruger, R. Goddard), Oxford University Press, Oxford (England), **1985** pp. 175–189.
[17] G. M. Sheldrick, SHELXL-93: Program for Crystal Structure Refinement, University of Göttingen (Germany), **1993**.
[18] L. Zsolnai, ZORTEP, An Interactive ORTEP Program, University of Heidelberg (Germany), **1994**.

Received: December 20, 2001 [F3750]